

RESOLVING VEGETATION CONDITION AND BIOGEOCHEMICAL PROCESSES USING HYPERSPECTRAL-BRDF INVERSE MODELING

Gregory P. Asner¹, C. Ann Bateson², Alan R. Townsend³, and Carol A. Wessman^{2,3}

1. INTRODUCTION

Complex variation in terrestrial biogeochemical cycles results from climatic, edaphic, biotic and human processes operating at multiple spatial and temporal scales. This variation cannot easily be resolved at the landscape, regional or global level without an integrated effort involving field research, modeling and remote sensing. To date, the role of remote sensing in terrestrial biogeochemical research has been limited to land-cover change analysis and estimation of two functional properties of vegetation: leaf area index (LAI) and fractional photosynthetically active radiation absorption (fAPAR). Traditional land-cover remote sensing provides the minimum information on the extent of major vegetation types needed to constrain ecosystem models to actual conditions (Wessman and Asner, 1997). Some ecosystem models also utilize remotely sensed estimates of LAI and fAPAR to derive plant carbon uptake or net primary productivity (NPP), which then feeds into soil carbon, nutrient and water algorithms that calculate a wide range of biogeochemical fluxes (Running et al, 1994; Field et al, 1995).

LAI and fAPAR estimates are currently made using the Normalized Difference Vegetation Index (NDVI), which is both theoretically and experimentally linked to the total chlorophyll and water content of plant canopies (Myneni and Williams, 1995; Gamon et al, 1996). However, observed changes in the NDVI cannot resolve differences in the relative importance of: (1) canopy chlorophyll and water content that occurs via changes in foliar properties and LAI, (2) vegetation structure which occurs via changes in horizontal cover and canopy architectural development, and (3) background albedo (e.g., soil and litter). At high spatial resolution (e.g., < 1km), each of these factors can vary enough to play an important role in determining pixel-level reflectance. For regional ecological and biogeochemical studies, additional information – beyond that which can be provided by the NDVI – is required to quantify the relative impact of these factors on remotely sensed optical data.

1.1 Sources of Variability in Vegetation Spectral Reflectance Data

The spectral, angular, spatial and temporal dependence of ecosystem (pixel level) reflectance (ρ_{pixel}) can be summarized in the relationship:

$$\rho_{\text{pixel}} = f(\text{GEOMETRY, STRUCTURE, BIOCHEMISTRY, GEOCHEMISTRY}) \quad (1)$$

GEOMETRY represents the solar and sensor viewing orientation. STRUCTURE includes canopy materials and architectural features such as the horizontal distribution of vegetation types, canopy height, canopy leaf and non-photosynthetic vegetation (NPV) area, leaf and NPV angular distributions, and foliage clumping.

BIOCHEMISTRY represents the chemical make-up of the tissues such as carbon, nitrogen and water content, while GEOCHEMISTRY includes the mineral and moisture content of surface soils.

Although some absorption features in the shortwave optical range can be attributed to any one of these factors, it is the combination of factors that gives rise to almost any given reflectance change in vegetated pixels. For example, the presence of chlorophyll results in a well-defined absorption feature at 680 nm, but remote sensing does not resolve changes in foliar chlorophyll. Rather it resolves canopy or pixel-level absorption at 680 nm, which occurs through a combination of foliar chlorophyll, canopy LAI, leaf orientation and canopy architectural development. This principle of multi-scale control on vegetation reflectance applies to pixel-level water and carbon content as well. Which factors in equation (1) exert the strongest control on the spectral, angular, spatial and temporal variability of vegetation reflectance in ecosystems? This is a critical question that needs to be answered

¹ Department of Geological and Environmental Sciences, Stanford University, Stanford, CA; Email: gpa@pangea.stanford.edu

² Cooperative Institute for Research in Environmental Sciences, University of Colorado, Boulder, CO; Emails: ann@cires.colorado.edu, wessman@cires.colorado.edu

³ Department of EPO Biology, University of Colorado, Boulder, CO; Email: townsenda@spot.colorado.edu

before remote sensing – the inverse to this question – can be employed for quantitative ecological and biogeochemical research.

In an effort to develop a quantitative understanding of the sources of variability in vegetation reflectance, we are compiling information on the ecological variability of each factor summarized in equation (1) across a wide range of ecosystems. We are developing a database of shortwave foliar, litter, wood and soil optical properties in an effort to quantify their importance at canopy and landscape levels. The first results from this effort are summarized in Asner et al (1997), Asner (1998) and Asner et al (1999); they show that in most ecosystems, variation in fully-developed, green-leaf optical properties plays a secondary role to structural attributes in driving pixel-level reflectance variation. An example of this is shown in Figure 1; leaf optical variability (leaf reflectance shown in panel A) does not give rise to significant canopy-level reflectance variability when canopy LAI < 5.0 (example with LAI = 1.5 shown in panel B). Similarly, in regions where a significant amount of standing litter (e.g., grasslands, shrublands, savannas) or woody material (e.g., deciduous forest) is exposed, variation in their tissue optical properties is conservative in comparison to ecological variability in the amount and architectural placement of the tissues (Figure 2). These and similar analyses provide a means to quantify the scale-dependent sources of variability in canopy reflectance data for any ecosystem represented our the tissue optical-canopy structural database.

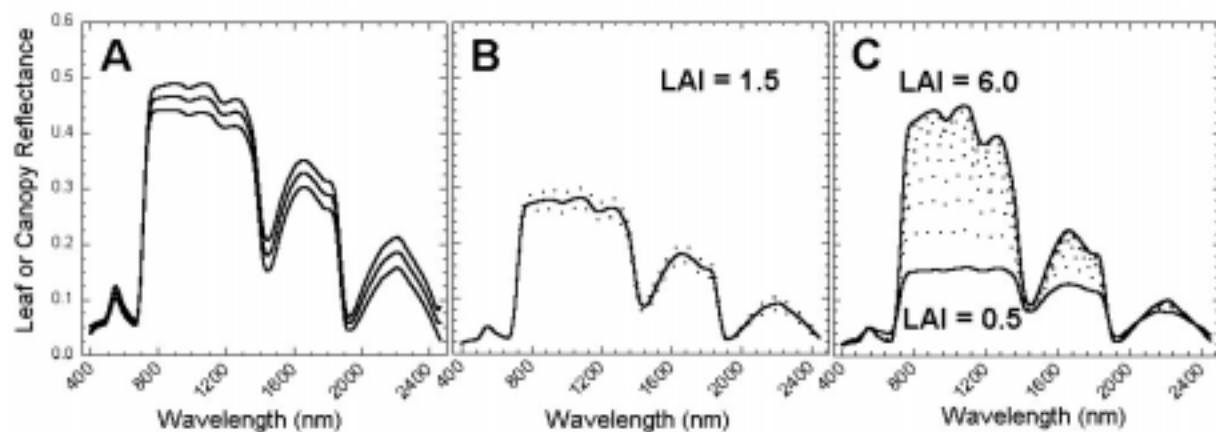


Figure 1. (A) Mean (± 1 s.d.) reflectance spectra of live foliage from our tissue optical database ($n = 1442$). (B) Effect of leaf optical variation from panel (A) on canopy-level nadir reflectance variation. Here, we used a canopy radiative transfer model (Shultis and Myneni 1988) to simulate a canopy with LAI = 1.5. (C) Variation in nadir canopy reflectance data due to changes in LAI (0.5-6.0). The mean leaf optical values from panel (A) were used here.

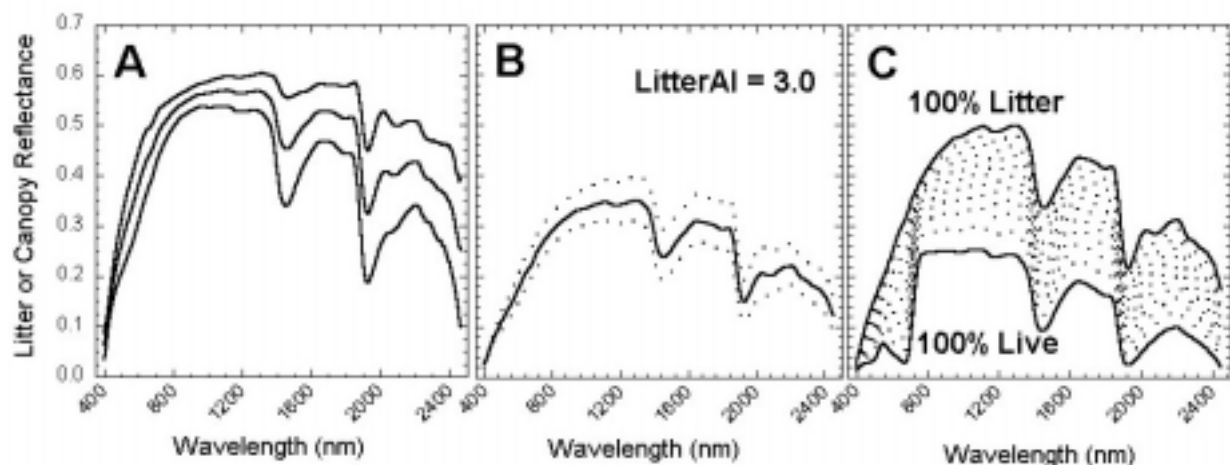


Figure 2. (A) Mean (± 1 s.d.) reflectance spectra of standing grass litter tissue from our database ($n = 304$). (B) Effect of litter optical variation from panel (A) on canopy-level nadir reflectance variation when litter area index (mm^2) or LitterAI = 3.0. (C) Variation in nadir canopy reflectance due to changes in the live:litter ratio of a typical grassland canopy. Mean litter optical properties from panel (A) were used here.

2.0 BIOPHYSICAL BASIS FOR RESOLVING CONTROLS ON SPECTRAL SIGNATURES

Compilation and analysis of tissue optical and canopy structural contributions to pixel reflectance provides a biophysical understanding of sources of variability. However, it does not provide a means to incorporate this *a priori* knowledge (either from field measurements or modeling) directly into the remote sensing process. The scale dependence of each factor involved (equation 1) complicates the link between remotely sensed signatures and any one factor alone. For example, changes in foliar or canopy chemistry cannot be easily evaluated against remote sensing data because the optical and structural attributes of vegetation and soils vary in three dimensional space and in time (Asner, 1998). Moreover, almost all ecological research involving remote sensing attempts to extrapolate point-level processes or characteristics to broad spatial scales, yet this activity also involves physical scaling in vertical space. A method that accounts for the scale dependence of tissue optical and canopy structural attributes is therefore needed.

Canopy photon transport models provide a physically consistent means to extend a field-level understanding of vegetation properties to a broader scale, and thus they allow for the spatial extrapolation of validation data to scales more commensurate with remotely sensed data. Beyond this level of integration, photon transport models also provide a means to improve remotely sensed measurements of vegetation by allowing *a priori* knowledge to constrain the physical interpretation of spectral, angular, temporal and spatial signatures. A diagrammatic representation of this process is shown in Figure 3. Remotely sensed data is used to assess the radiative characteristics of each pixel using a photon transport model. Biogeophysical information, such as soil optical variability or tissue reflectance relationships between spectral bands (Asner et al, 1998), provides constraint of the model while combinations of unknown factors (e.g. leaf area, live:dead fraction, bare soil extent) are simulated. These combinations are compared, and the best match between measured and modeled values provides an estimate of the canopy properties of interest.

Once the canopy variables are estimated, these can be used to calculate plant functional properties such as energy absorption (again using a photon transport model; Asner and Wessman, 1997) and ecological processes such as carbon uptake and evapotranspiration (using an ecosystem or land-surface model; Field et al, 1995; Sellers et al, 1997). One of the most powerful aspects of this approach is that uncertainty in the remote sensing data, field measurements, landscape assumptions, and models can be accounted for explicitly at each step of the process. For example, uncertainty in the model constraints provided by field measurements can be evaluated using Monte Carlo analysis, providing a range and probability distribution of retrieved canopy values. This approach allows for the propagation of uncertainty from remote sensing data to ecological processes (Figure 3).

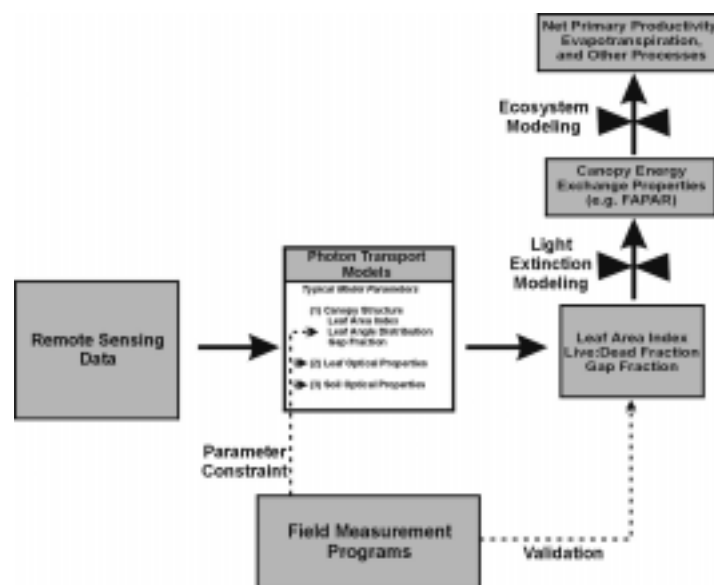


Figure 3. Photon transport models provide a means to incorporate *a priori* biophysical and ecological knowledge directly into the remote sensing process. Field measurements can thus be used in a physically consistent way to constrain remote sensing estimates and/or validate them (from Asner 1999).

2.1 Photon Transport Inverse Modeling

Based on the biophysical scheme for incorporating *a priori* information into the remote sensing process (Figure 3), how does one find the combination of variables (equation 1) that produces simulated reflectance values best matching the observational data? The photon transport inverse modeling (PTIM) approach fits most directly into the process by minimizing the difference between measured and modeled reflectance values using an optimization routine (Figure 4). The approach is robust in that it provides a consistent means to integrate *a priori* knowledge as described earlier, and it allows any combination of variables that are within the domain of ecological and biophysical plausibility as determined by the researcher. In other words, the expert knowledge of the researcher limits the domain of possible values searched. A simple example would be to limit the brightness of the background soil based on surface soil mineralogical maps and spectral measurements of those soil types.

Another robust characteristic of the PTIM approach is that it explicitly accounts for the anisotropic reflectance behavior of vegetation and soils (Goel, 1988; Privette et al, 1996). Variation in canopy gap fraction, leaf angle distribution and canopy height result in significant non-Lambertian behavior of vegetation reflectance signatures (e.g., Li et al, 1995). Angular dependence of surface reflectance is usually handled as residual signal, and attempts are made to remove it as noise (Kennedy et al, 1997). The PTIM approach resolves this problem by physically accounting for reflectance anisotropy; that is, the model uses the known solar and viewing geometry in providing the canopy reflectance estimates. In fact, many studies have shown that the angular reflectance signature is a good source of information for estimating vegetation macro-structural properties (e.g., gap fraction) as well as for quantifying atmospheric contributions (e.g., aerosol) to a top-of-atmosphere radiance measurement (e.g., Privette et al, 1996).

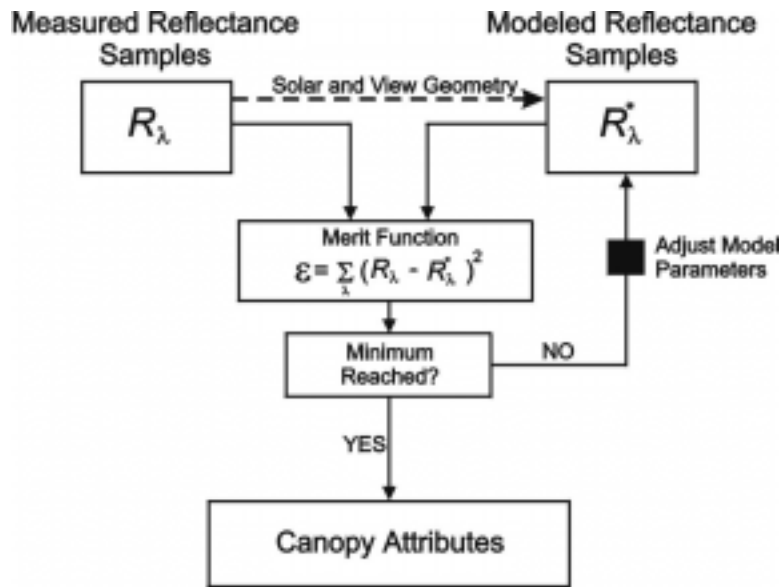


Figure 4. Photon transport inverse modeling allows for canopy attributes of interest (e.g. Figure 3) to be estimated by minimizing the difference between measured and modeled reflectance values. The model parameters leading to this minimum difference are considered the retrieved attributes. A merit function lies at the center of the inversion approach and is used to evaluate the minimum. Any one of a variety of optimization routines (e.g., quasi-newton minimizer, genetic algorithms) can be used to locate the global minimum.

Although these attributes make the PTIM approach robust for remote sensing analysis, it can also be problematic for several reasons. First, the photon transport model may not adequately account for all of the physical processes involved, and thus an accurate solution via model inversion may not be obtainable. The severity of this particular problem has been decreasing over the last several years as more sophisticated representations of the biogeophysical environment affecting the radiation field have been developed (e.g., Myneni and Asrar, 1993; Gobron et al, 1997). Nonetheless, this is a persisting problem which must be addressed using a combination of field and modeling analyses as discussed in Section 1.1.

A second major weakness of the PTIM approach lies in having insufficient data to execute the inversion. This problem usually occurs when the model is insufficiently sensitive to data characteristics (e.g., certain spectral wavelengths or viewing angles) and/or when the data do not provide sufficiently unique information needed to solve for a single vegetation parameter set (the global minimum). Again, these problems are addressed via an integrated field and modeling approach; the more constraints that can be put on the inversion without compromising the general applicability of the algorithm for its application (e.g., landscape, region, time of year), the better one's chance of finding the correct, unique solution to the inverse problem.

2.2 Hyperspectral Data: Sufficient for Canopy Inverse Modeling Methods?

Does a hyperspectral signature contain sufficient information to execute the inverse modeling approach described in Section 2.1? The answer to this question lies in the level of field and modeling integration (e.g., Figure 3) used to develop the domain of ecologically and biophysically plausible solutions. The answer is also dependent upon the quality of the remote sensing measurements and the accounting of atmospheric constituents (e.g., aerosols, cirrus clouds). In the following case studies, we use the integrated approach, including photon transport inverse modeling techniques, to estimate ecologically and biogeochemically important variables in land-use systems of the Southwest U.S. and Amazon Basin. We show that hyperspectral data provides sufficient information to estimate ecologically important variables while accounting for biogeophysical properties of less interest.

3.0 CASE STUDIES OF LAND USE CHANGE

The following examples show how an understanding of biophysical sources of variability in vegetation reflectance spectra can be integrated with the PTIM method to estimate the following three variables:

- plant area index (total projected area of plant material per unit ground area; m^2m^{-2})
- live:dead fraction of biomass
- bare soil cover (%)

These variables can then be used to estimate important functional processes such as fAPAR, carbon and nutrient uptake and decomposition in biogeochemical analyses (Asner, 1999).

3.1 Biogeochemical Processes in Subtropical Savannas

3.1.1 Study Site

The Texas A&M La Copita Research Area is located on the Rio Grande Plains of southern Texas (27°40'N, 98°12'W), roughly 80 km west of Corpus Christi. Like many regions of the western United States, the area has endured over a century of heavy grazing and fire suppression, leading to the encroachment of woody plant species into ecosystems once dominated by grasses (Archer, 1995). Micro-topographical and physical soil variation result in a polygonal-reticulate patterning of vegetation across the landscape (Figure 5). Woody plant canopies are dominated by the leguminous tree *Prosopis glandulosa* var. *glandulosa*, with many secondary shrubs, all imbedded in an herbaceous cover dominated by C_4 grasses. The structural attributes of woody plant canopies (size, LAI, extent) reflect both natural variability and time since woody cluster establishment (Archer, 1995). Playas, which occur on large shallow depressions found in the woodland areas, are prone to flooding during rainfall events, and are dominated by tall C_4 grasses with dispersed trees. In addition, large monospecific fields of *Cenchrus ciliaris* (buffleggrass) and *Cynodon dactylon* (coastal bermudagrass) are present in the area.

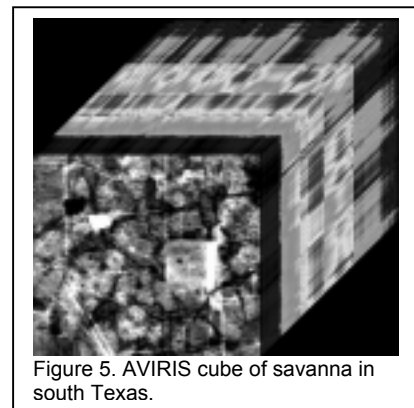


Figure 5. AVIRIS cube of savanna in south Texas.

3.1.2 AVIRIS Data

AVIRIS imagery was acquired over the La Copita Research Area on 8 August 1993 (Figure 5). AVIRIS was flown on an ER-2 aircraft at an altitude of 20 km and acquired spectral data in 224 channels in the shortwave spectrum (400-2500 nm). Upwelling radiation from the earth's surface was measured at a spatial resolution of 20 m

and with ground coverage of approximately 120 km². Measured radiance values were reduced to apparent surface reflectance using a solar and atmospheric model (ATmospheric REMoval Model [ATREM]; Gao et al, 1993). The AVIRIS channels affected by strong atmospheric water absorption (centered on 1400 and 1900 nm) were removed, yielding 179 spectral bands for subsequent analyses.

3.1.3 Photon Transport Inverse Modeling

We used a discrete ordinates model to simulate the interaction of solar energy with the plant canopies (Asner et al, 1998). Jaquinta and Pinty (1994) developed the computationally efficient multiple-scattering approximation, which allowed us to use an accurate multi-stream calculation with the data-rich AVIRIS spectra. Our model formulation includes both leaf and non-photosynthetic vegetation (NPV) (Qin, 1993). It is designed explicitly for use with hyperspectral data, as wavelength-independent calculations are made only once per simulation, while wavelength-specific calculations are iterated for each AVIRIS channel. The model produces top-of-canopy AVIRIS reflectance spectra from the these variables: leaf and NPV area index (LAI, NPVAI), leaf and NPV angle distributions, percent vegetation cover, tissue reflectance and transmittance properties, soil reflectance, and sun and viewing orientation.

For each image pixel, the model was inverted using the 179 AVIRIS channels which provided near-continuous shortwave spectral coverage. We showed that AVIRIS data contain regions where both the magnitude and shape (first derivatives) of the reflectance spectra are highly sensitive to leaf, woody stem, and litter content (LAI, NPVAI) (Asner, 1998). First derivative spectra were weakly sensitive to variation in tissue scattering properties in canopies with LAI < 5, which are typical of arid and semi-arid ecosystems. Therefore, tissue optical properties were held constant to the mean reflectance and transmittance spectra of a large foliar and NPV data set collected from sites in the southwest United States (Asner et al, 1998).

Both the extent of vegetation cover and soil reflectance strongly influence the spectral reflectance characteristics of arid and semi-arid ecosystems (Huete, 1988; van Leeuwen and Huete, 1996). Inversion of a photon transport model in these regions thus requires *a priori* knowledge of these factors; this can be acquired directly from imaging spectrometer data via spectral mixture analysis. Spectral mixture analysis is a method by which the relative contribution of land covers are quantified within image pixels, and the fraction of vegetation cover and exposed soils within image pixels can be estimated with high accuracy using imaging spectrometer data. Wessman et al (1997) spectrally unmixed the AVIRIS image using the method of Bateson and Curtiss (1996), yielding bare soil cover fractions within image pixels which were used to fix the vegetation cover parameter in the model inversions. A summary of the canopy model parameters, constraints on some of these parameters, and the sources of information for these constraints is provided in Table 1.

Table 1. Summary of hyperspectral photon transport model parameters and constraints during model inversions.

Model Parameter	Constraint in Inversion	Source
Leaf Area Index	None	---
NPV Area Index	None	---
Leaf Angle Distribution	plagiophile	Myneni et al (1989)
NPV Angle Distribution	erectophile	Myneni et al (1989)
Tissue optical properties	Spectra in 179 AVIRIS optical channels fixed to mean values from field survey	Asner et al (1998)
% vegetation cover	Spectral mixture analysis of AVIRIS data	Wessman et al (1997) Bateson and Curtis (1996)
Soil reflectance	Spectral mixture analysis of AVIRIS data	Wessman et al (1997) Bateson and Curtis (1996)
Solar geometry	Zenith = 22.5°, Azimuth = 116.3°	AVIRIS ephemeris data
Viewing geometry	varies with across-track pixel location	AVIRIS specifications

In each pixel, a quasi-newton optimization procedure (Numerical Algorithms Group Ltd.) was used to minimize the difference between measured (AVIRIS) and modeled canopy reflectance. This procedure iterates forward model calculations until the merit function, representing this difference, converges on a minimum value (Figure 4). The method requires a starting point for all model parameters which, in an ill-conditioned mathematical situation, can lead to the entrapment of the optimizer in a local minimum (as opposed to the desired global

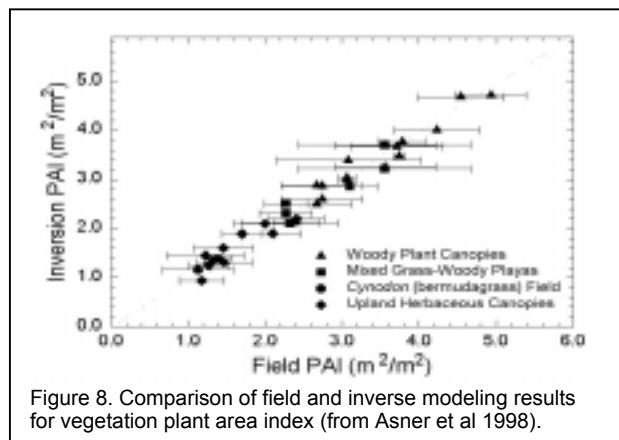
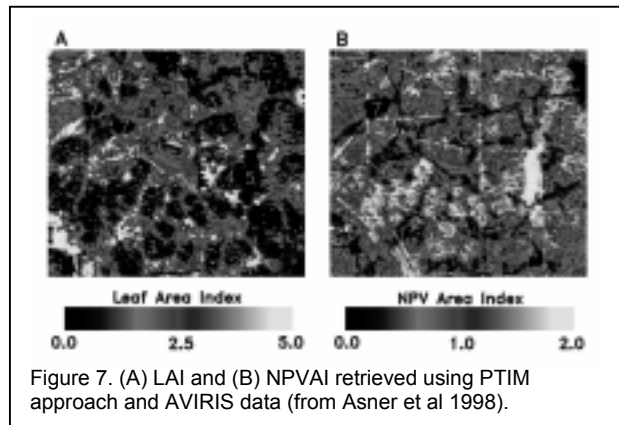
minimum). To safeguard against local entrapment, the inversion was repeated three times. Random values were added to the parameters retrieved in the first inversion, and the optimizer was restarted from that point. The procedure was then repeated a third time. Our experience indicated that three restarts is a sufficient precaution to ensure that the global minimum is reached.

3.1.4 Results

Almost all of the AVIRIS pixel inversions converged to a solution (40,881 of 41,065 pixels) and adequately minimized the merit function. Those inversions not producing a solution coincided with a small cluster of cloudy pixels. For each of the three inversion attempts on a pixel, the minimization routine always converged to the same result, suggesting that the method produced unique solutions. Merit function values for the successful inversions ranged from 0.004-0.085, with a mean (± 1 s.d.) = 0.016 (0.007). The root-mean-square error (RMS) ranged from 1-2%, indicating a reasonable fit between measured and modeled spectra (Privette et al, 1996).

August is the dry season in southern Texas, so herbaceous canopies were dominated by standing grass litter. Trees and shrubs were close to maximum greenness, with full leaf display and little to no senescent material in the canopy. Landscape patterns of woody plant and senescent herbaceous vegetation are shown in the retrieved LAI and NPVAI values (Figure 7).

The results were evaluated against plant area index ($PAI = LAI + NPVAI$) measurements acquired in the field. An area-weighting method was used to scale canopy PAI measurements to the AVIRIS pixel level through estimates of woody plant and herbaceous cover derived from high resolution aerial photographs and transect surveys. These area-weighted field measurements were co-registered to the AVIRIS data (69 pixels) using differentially-corrected GPS with sub-meter accuracy. In pixels dominated by woody plant cover, field PAI measurements had a mean (± 1 s.d.) = 3.5 (0.8). The sum of the leaf and NPV area index results from the model inversions (Figure 7a+7b) produced a very similar distribution of woodland PAI estimates: mean (± 1 s.d.) = 3.3 (0.7). Leaf and NPV area estimates for grass-dominant canopies were also in close agreement with field observations. Ground-based PAI measurements ranged from 1.2 to 2.5, with a mean (± 1 s.d.) = 1.7 (0.3), while PAI values derived through inverse modeling ranged from 1.1 to 2.3, with a mean (± 1 s.d.) = 1.5 (0.4). Pixel-to-pixel comparisons demonstrated excellent agreement between ground and remotely sensed PAI values (Figure 8). Absolute errors ranged from 0.0-0.4 PAI, with a mean error (± 1 s.d.) = 0.2 (0.1). Mean (± 1 s.d.) relative RMS error was 8(5)%.



3.2 Pasture Condition in the Amazon Basin

3.2.1 Study Site

Land use in the Amazon Basin is dominated by cattle ranching, yet the sustainability of ranching in this region has long been questioned. The low nutrient status of the Amazon's highly weathered soils leads to pasture degradation within 5-15 years after the initial clearing, resulting in continual clearing and increasing rates of deforestation. However, both the exact cause of pasture degradation is not clear and the regional patterns of pasture productivity, degradation, and thus carbon and nutrient cycles are difficult to assess. We established a pasture age

and soil texture gradient in the central Amazon (south of Santarem; 3°30'S, 55°00'W) to study nutrient and carbon dynamics in conjunction with remotely sensed spectral signatures of pasture degradation.

3.2.2 Remote Sensing Data

To date, most remote sensing involving the process of forest-to-pasture conversion has relied on Landsat or similar multi-spectral data to estimate pasture age and secondary regrowth (e.g., Skole and Tucker, 1993). Remote sensing has not often been used to estimate biophysical properties such as LAI, litter fraction or bare soil extent because insufficient information may be contained in standard 6-channel broadband signatures. Less attention has focused on the use of hyperspectral data to assess pasture condition, yet this may be the most promising method if both PAI (= LAI+NPVAI) and the live:dead fraction of the pasture grasses can be estimated. Because most of the Amazon experiences heavy cloud cover but a pronounced dry season, short windows of opportunity become available for gathering biophysical information using remote sensing. These dry-season windows occur between August and November when pasture grasses are moderately to highly senescent. The live plus standing dead (or senescent) material (PAI) primarily indicates growth during the last rainy season, some of which senesces during the dry season. Resolving pasture condition therefore requires estimation of both live and senescent material.

AVIRIS and other airborne imaging spectrometer data were not available during our field campaigns in 1997 and 1998, therefore we used ground-based spectrometer data to assess its utility for measuring pasture canopy biophysical properties. We used a full spectral range (400-2500 nm) spectrometer (Analytical Spectral Devices, Inc.) with the sensor optic located 1 m about ground level and positioned at nadir. We collected data in 0.5 m increments along 100 m transects, and converted the radiance measurements to surface reflectance using a calibration panel. We collected simultaneous canopy structural, foliar optical, and soil spectral measurements as well as a suite of soil nutrient and carbon measurements.

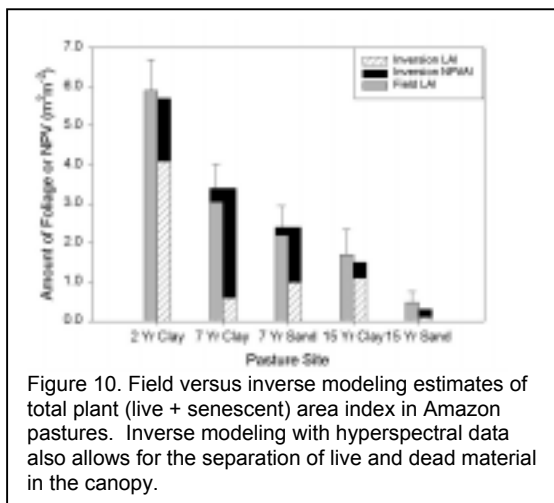
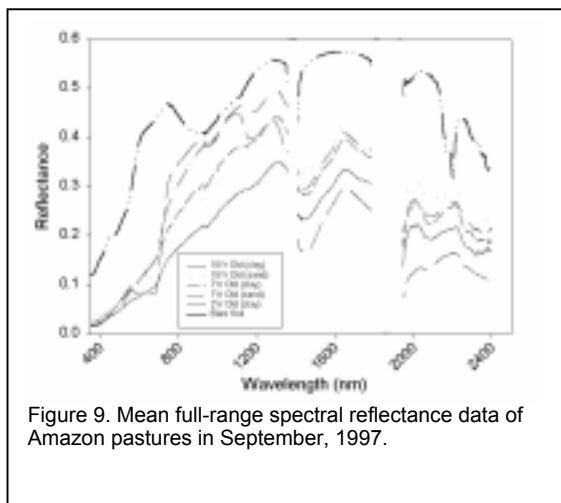
3.2.3 Photon Transport Inverse Modeling and Constraints

The PTIM approach was used to estimate LAI, live:dead fraction and bare soil extent in each pasture along the chronosequence (2, 7 and 15 years old on sand and clay soils). We constrained the model to mean values of leaf optical properties of the two dominant grasses found in pastures throughout the region: *Brachyaria brizantha* and *Pennesetum penniculatum*, and we constrained the soil optics to a range of possible values from soils collected in the region. Photon transport model inversion was carried out as shown in Figure 4.

3.2.4 Results

Mean spectral reflectance values are shown in Figure 9. Distinction differences in pasture condition can be resolved in two optical regions of the shortwave spectrum. The visible/near-IR region indicates variation in live foliar content, which is correlated with canopy chlorophyll content. The shortwave-IR region (1700-2400 nm) contains several features associated with standing litter fraction. Although several absorption features indicate biogeophysical differences among the pastures, it is the overall shape of the spectra (e.g., via first derivatives) that make them quantitatively distinct (Asner, 1998).

Using the reflectance continuum information, we inverted the photon transport model and estimated LAI and live:dead fraction (Figure 10). Bare soil was nearly zero in all pastures; this agreed with our field observations.



LAI did not decrease consistently with pasture age and coarser soil texture, but the total live+dead biomass did decrease dramatically. As noted earlier, the total biomass indicates growth in previous growing seasons, but the live fraction may not. Rather, live fraction may indicate both growth and time since last rainfall in a particular pasture.

This level of detail is difficult to achieve using multi-spectral measurements because broadband measurements (e.g., Landsat TM) cannot easily distinguish between bare soil and litter, which look similar in the visible/near-IR spectrum (data not shown). An adequate sampling of the shortwave-IR is required to distinguish the contribution of soils and senescent vegetation material (Asner et al, 1999).

4.0 CONCLUSIONS

The biophysical integration scheme presented here, in conjunction with the photon transport inverse modeling approach, provides a physically consistent means to estimate ecologically important information from hyperspectral signatures. It is a robust approach for simulating remotely sensed signatures of vegetation and soils; it provides a means to scale, in three-dimensional space, from leaf to landscape level. The most powerful characteristic of the approach is that it allows a consistent integration of ecological and physical knowledge at all stages of the remote sensing process, providing a means to estimate and propagate error from radiance data to retrieved ecological parameter.

In the few case studies highlighted here, the PTIM method allowed us to estimate ecological variables of interest with high accuracy. We incorporated some *a priori* knowledge on tissue optical properties, which we have found to vary conservatively within and between ecosystem types, and soil optics, which can be constrained to relatively narrow ranges based on field measurements and maps. Further work is needed to assess the applicability of the approach across many biome types and under varying ecological and biophysical conditions. We predict that the general framework presented here will be applicable to any ecosystem, but that the constraints, and thus the breadth of parameters that can be retrieved, will be ecosystem dependent. We contend that hyperspectral data provide the best means to estimate most of the canopy variables of interest to ecological and biogeochemical research efforts (with the exception of gap fraction, which can be assessed using multi-angle data). Further work is underway to test these methods in a variety of ecosystems and a range of vegetation types.

5.0 ACKNOWLEDGEMENTS

This work has been supported in part by NASA IDS grant NAGW-2662, NASA Land-cover/land-use Change grant NAGW-6134, NASA NIP grant NAGW-5253, and the NASA Earth System Science Fellowship Program.

6.0 REFERENCES

- Archer, S., 1995, "Tree-grass dynamics in a Prosopis-thornscrub savanna parkland: reconstructing the past and predicting the future", *Ecosci.* 2:83-99.
- Asner, G.P. and C.A. Wessman, 1997, "Scaling PAR absorption from the leaf to landscape level in spatially heterogeneous ecosystems", *Ecol. Mod.* 103:81-97.
- Asner, G.P., et al., 1998, "Variability in leaf and litter optical properties: implications for canopy BRDF model inversions using AVHRR, MODIS, and MISR", *Remote Sens. Environ.* 63:200-215.
- Asner, G.P., 1998, "Biophysical and biochemical sources of variability in canopy reflectance", *Remote Sens. Environ.* 64:234-253.
- Asner, G.P., C.A. Wessman, and D.S. Schimel, 1998, "Heterogeneity of savanna canopy structure and function from imaging spectrometry and inverse modeling", *Ecol. Applic.* 8:926-941.
- Asner, G.P., et al., 1999, "Impact of Tissue, Canopy and Landscape Factors on Reflectance Variability of Arid Ecosystems", *Remote Sensing of Environment*. In press.
- Asner, G.P., 1999, "Ecological and biogeochemical analysis of arid and semi-arid regions in the EOS era Remote Sens. Environ. In press.
- Bateson, C.A. and B. Curtiss, 1996, "A method for manual endmember selection and spectral unmixing", *Remote Sens. Environ.* 55:229-243.

- Field, C.B., J.T. Randerson, and C.M. Malmstrom, 1995, "Global net primary production: combining ecology and remote sensing", *Remote Sens. Environ.* 51:74-88.
- Gamon, J.A., et al., 1995, "Relationships between NDVI, canopy structure, and photosynthesis in three Californian vegetation types", *Ecol. Appl.* 5:28-41.
- Gao, B.-C., K.B. Heidebrecht, and A.F.H. Goetz, 1993, "Derivation of scaled surface reflectance from AVIRIS data", *Remote Sens. Environ.* 44:165-178.
- Gobron, N., B. Pinty, and Y. Govaerts, 1997, "A semi-discrete model for the scattering of light by vegetation", *J. Geophys. Res.* 102:9,431-9,445.
- Goel, N.S., 1988, "Models of vegetation canopy reflectance and their use in estimation of biophysical parameters from reflectance data", *Remote Sens. Rev.* 4:1-212.
- Huete, A.R., 1988, "A soil-adjusted vegetation index (SAVI)", *Remote Sens. Environ.* 25:295-309.
- Iaquinta, J. and B. Pinty, 1994, "Adaptation of a bidirectional reflectance model including the hotspot to an optically thin canopy", *Proc. Sixth Int'l Symp. Phys. Measur. and Signatures Remote Sens.*, pp. 683-690.
- Kennedy, R.E., W.B. Cohen, and G. Takao, 1997, "Empirical methods to compensate for a view-angle-dependent brightness gradient in AVIRIS imagery", *Remote Sens. Environ.* 62:277-286.
- Li, X., A.H. Strahler, and C.E. Woodcock, 1995, "A hybrid geometric optical-radiative transfer approach for modeling albedo and directional reflectance of discontinuous canopies", *IEEE Trans. Geosci. Remote Sens.* 33:466-480.
- Myneni, R.B. and G. Asrar, 1993, "Radiative transfer in three-dimensional atmosphere-vegetation media", *J. Quant. Spectrosc. Radiat. Trans.* 49:585-598.
- Myneni, R.B., J. Ross, and G. Asrar, 1989, "A review on the theory of photon transport in leaf canopies", *Agric. For. Meteorol.* 45:1-153.
- Myneni, R.B. and D.L. Williams, 1994, "On the relationship between fAPAR and NDVI", *Remote Sens. Environ.* 49:200-209.
- Privette, J.L., W.J. Emery, and D.S. Schimel, 1996, "Inversion of a vegetation reflectance model with NOAA AVHRR data", *Remote Sens. Environ.* 58:187-200.
- Qin, W., 1993, "Modeling bidirectional reflectance of multicomponent vegetation canopies", *Remote Sens. Environ.* 46:235-245.
- Running, S.W., T.R. Loveland, and L.L. Pierce, 1994, "A vegetation classification logic based on remote sensing for use in global biogeochemical models", *Ambio* 23:77-89.
- Sellers, P.J., et al., 1997, "Modeling the exchanges of energy, water, and carbon between continents and the atmosphere", *Science* 275:502-509.
- Skole, D. and C. Tucker, 1993, "Tropical Deforestation and Habitat Fragmentation in the Amazon: Satellite Data from 1978 to 1988", *Science* 260:1905-1908.
- van Leeuwen, W.J.D. and A.R. Huete, 1996, "Effects of standing litter on the biophysical interpretation of plant canopies with spectral indices", *Remote Sens. Environ.* 55:123-134.
- Wessman, C.A. and G.P. Asner, 1998, Ecosystems and the problems of large-scale measurements, Pages 346-371 in: P. Groffman and M. Pace, editors. *Successes, Limitations, and Frontiers in Ecosystem Ecology*. Springer-Verlag, Berlin.
- Wessman, C.A., et al., 1998, "A method to access absolute fIPAR of vegetation in spatially complex ecosystems", *Proc. 7th Ann. Airborne Earth Sci. Workshop*.